THE JOURNAL OF PHYSICAL CHEMISTRY A

Article

Self-Consistent Field Calculations of Excited States Using the Maximum Overlap Method (MOM)

Andrew T. B. Gilbert, Nicholas A. Besley, and Peter M. W. Gill

J. Phys. Chem. A, **2008**, 112 (50), 13164-13171 • Publication Date (Web): 26 August 2008

Self-Consistent Field Calculations of Excited States Using the Maximum Overlap Method (MOM)†

Andrew T. B. Gilbert,*,‡ Nicholas A. Besley,§ and Peter M. W. Gill‡

Research School of Chemistry, Australian National University, ACT 0200, Australia, and School of Chemistry, University of Nottingham, Nottingham NG7 2RD, England

Received: February 28, 2008; Revised Manuscript Received: June 19, 2008

We present a simple algorithm, which we call the maximum overlap method (MOM), for finding excited-state solutions to self-consistent field (SCF) equations. Instead of using the aufbau principle, the algorithm maximizes the overlap between the occupied orbitals on successive SCF iterations. This prevents variational collapse to the ground state and guides the SCF process toward the nearest, rather than the lowest energy, solution. The resulting excited-state solutions can be treated in the same way as the ground-state solution and, in particular, derivatives of excited-state energies can be computed using ground-state code. We assess the performance of our method by applying it to a variety of excited-state problems including the calculation of excitation energies, charge-transfer states, and excited-state properties.

1. Introduction

The time-independent Schrödinger wave equation for an n-electron system

$$\hat{H}\Psi_k = E_k\Psi_k \tag{1.1}$$

is the foundation of quantum chemistry. The Ψ_k are wave functions of the stationary states of the system, and the E_k are their energies. The Hamiltonian operator $\hat{H}$ is Hermitian and its eigenfunctions Ψ_k form a complete, orthogonal basis for n-particle space.

Obtaining accurate solutions of (1.1) is onerous, and this difficulty has spawned a wide variety of methods for obtaining approximate solutions. One of the most successful strategies is to approximate $\hat{H}$ by a sum of one-electron operators

$$\hat{H}^{\mathrm{SCF}} = \sum_{i=1}^{n} \hat{f}(r_i) \tag{1.2}$$

because the eigenfunctions of the resulting simplified Schrödinger equation

$$\hat{H}^{\mathrm{SCF}}\Psi_k^{\mathrm{SCF}} = E_k^{\mathrm{SCF}}\Psi_k^{\mathrm{SCF}} \tag{1.3}$$

are just single determinants

$$\Psi_k^{\mathrm{SCF}} = \det[\chi_i(r_j, s_j)] \tag{1.4}$$

where the $\chi_i(\mathbf{r},s) = \psi_i(\mathbf{r})\sigma(s)$ are spin−orbitals and each molecular orbital (MO)

$$\psi_i(\mathbf{r}) = \sum_{\mu}^{N} C_{\mu i}\phi_\mu(\mathbf{r}) \tag{1.5}$$

is expanded in a finite basis $\{\phi_\mu\}$.

In the most accurate schemes,[1−4] $\hat{H}^{\mathrm{SCF}}$ depends on its eigenfunction Ψ_i^{SCF} and (1.3) is therefore nonlinear and requires iterative solution.[5] The MO coefficients $C_{\mu i}$ are usually determined by minimizing the energy using one of several procedures[6−11] and this process is continued until $\hat{H}^{\mathrm{SCF}}$ and Ψ_i^{SCF} converge, at which point a self-consistent field (SCF) has been achieved. This usually yields the lowest-energy single determinant within the basis.

The conceptual and computational simplicity of the one-electron model (1.2), together with its surprisingly high accuracy, has led to its widespread adoption for the treatment of ground states. In particular, Kohn−Sham density functional theory (DFT)[3,4] has become an extremely popular tool in quantum chemistry.

Long after HF and DFT were established for ground states, CIS (single-excitation configuration interaction[12,13]) and TD-DFT (time-dependent density functional theory[14,15]) were developed to provide broadly analogous treatments for excited states. Both extensions give qualitative and sometimes quantitative accuracy for low-lying valence excitation energies. However, CIS and TD-DFT do not allow relaxation of the orbitals in the excited state and they therefore fail where this relaxation is important. TD-DFT also inherits the deficiencies of the approximate functional used to compute the exchange-correlation component of the energy. TD-DFT performs particularly poorly for Rydberg states unless the exchange-correlation potential is patched,[16−18] and it fails to capture the correct behavior of charge-transfer excitations.[19,20] For such cases, more accurate (but significantly more expensive) approaches such as the complete active space self-consistent field (CASSCF),[21,22] the equation-of-motion coupled-cluster (EOM-CC),[23] and the spin-flip coupled-cluster (SF-CC)[24] methods can be used to obtain greater accuracy.

One may reasonably ask, however, whether it is either necessary or desirable to treat ground and excited states as if they were fundamentally different. Such a methodological discontinuity is difficult to justify on either physical or mathematical grounds and, indeed, by singling out the ground state for special treatment, we introduce a bias that can be hard to remove later. Is it not more natural, one may wonder, to obtain excited states by an SCF procedure?

After a ground-state SCF has converged, crude approximations to excited states can be obtained by promoting electrons

* Corresponding author. E-mail: andrew.gilbert@anu.edu.au.
† Part of the "Sason Shaik Festschrift".
‡ Australian National University.
§ University of Nottingham.

10.1021/jp801738f CCC: $40.75
Published on Web 08/26/2008

from occupied to virtual orbitals to yield singly- or multiply-excited states. This approach has well-known deficiencies, the most obvious of which is that the orbitals are optimal only for the ground state and are not able to relax after the electronic excitation. Indeed, the virtual orbitals feel the interaction of all n electrons in the system and are therefore more appropriate for excited states of the $(n + 1)$-electron system. In separate studies, Hunt and Goddard[25] and Huzinaga and Arnau[26,27] suggested methods for optimizing these virtual orbitals for excited states of the original n-electron system. They allow rotations within the virtual manifold but do not permit the occupied orbitals to relax. Morokuma and Iwata[28] later removed this constraint and allowed both the occupied and virtual orbitals to relax within their respective subspaces. In both cases, mixing between the occupied and virtual subspaces is forbidden and this ensures that the resulting excited states are rigorously orthogonal to the ground state. More recently, ensemble methods have been proposed wherein a weighted sum of the energies of the ground and singly excited determinants is minimized.[29] This yields a single set of orbitals that are a compromise between modeling the ground and excited states.

Such methods yield approximate excited states which are guaranteed to be orthogonal to the corresponding approximate ground state but which are no longer solutions of the SCF equations. We contend, however, that the importance of orthogonality has been overstated. Quantum mechanics requires exact wave functions to be orthogonal, i.e., $\langle\Psi_i|\Psi_j\rangle = 0$, $i \neq j$, but it makes no such demand on SCF wave functions and, in fact, one should expect $\langle\Psi_i^{\mathrm{SCF}}|\Psi_j^{\mathrm{SCF}}\rangle \neq 0$. Indeed, enforcing orthogonality to an approximate wave function serves only to propagate its shortcomings to other approximate wave functions. With this in mind, we will abandon orthogonality and, instead, seek genuine higher-energy solutions of the SCF equation (1.3) and use these as models for the excited states of the system.

The existence of such solutions has been proven under modest assumptions.[30] Furthermore, if a finite basis is introduced, the number of solutions can be very large; for example, with N basis functions there may exist $O(3^N)$ distinct, self-consistent solutions to the closed-shell, two-electron problem.[31] But, do the higher solutions have physical significance? The lowest eigenvalues of $\hat{H}$ and $\hat{H}^{\mathrm{HF}}$ typically differ by less than 1% and it is largely for this reason that HF theory ("the orbital approximation") has become the cornerstone of electronic structure theory. We conjecture that this similarity also holds for many of the higher eigenvalues and that the higher SCF solutions may be useful approximations to the corresponding excited states. Of course, SCF methods perform less satisfactorily for ground states with multideterminant character and we expect that this will also be true for the higher-energy solutions.[32]

The higher solutions, however, are difficult to obtain in practice because, as noted above, most SCF algorithms are designed to find the lowest-energy solution. This presents an interesting challenge: is there an inexpensive systematic algorithm for finding the higher solutions of the SCF equation (1.3)? In the remainder of this Paper, we present and test a simple protocol for choosing which orbitals to occupy at each iteration of an SCF calculation, in order that a target SCF solution emerges. The method, which is an alternative to the aufbau protocol, guards against variational collapse to lower-energy solutions of the same symmetry and frequently yields SCF solutions that are difficult or impossible to find using traditional SCF algorithms. We discuss the method in Section 2 and apply it to a variety of problems including the calculation of excitation energies, charge-transfer states, and excited-state properties in Section 3. Spin-unrestricted calculations are used throughout.

2. Maximum Overlap Method

On each iteration of the SCF procedure, the current MO coefficient matrix $\mathbf{C}^{\mathrm{old}}$ is used to build a Fock (or Kohn−Sham) matrix $\mathbf{F}$ and the generalized eigenvalue problem

$$\mathbf{FC}^{\mathrm{new}} = \mathbf{SC}^{\mathrm{new}}\varepsilon \tag{2.6}$$

(where $\mathbf{S}$ is the basis function overlap matrix) is then solved to obtain a new MO coefficient matrix $\mathbf{C}^{\mathrm{new}}$ and orbital energies ε. At that point, there are ${}^{N}C_{n}$ ways to choose which of the new orbitals to occupy but this large space is rarely, if ever, explored exhaustively. Instead, one usually follows the aufbau protocol, which dictates that one simply occupies the n orbitals with the lowest orbital energies ε_j.

An alternative protocol, which we call the maximum overlap method (MOM), states that the *new occupied orbitals should be those that overlap most with the span of the old occupied orbitals*. If we define the orbital overlap matrix

$$\mathbf{O} = (\mathbf{C}^{\mathrm{old}})^{\dagger}\mathbf{SC}^{\mathrm{new}} \tag{2.7}$$

then O_{ij} is the overlap between the ith old orbital and the jth new orbital, and the projection of the jth new orbital onto the old occupied space is

$$p_j = \sum_{i}^{n} O_{ij} = \sum_{\nu}^{N}\Big[\sum_{\mu}^{N}\Big(\sum_{i}^{n} C_{i\mu}^{\mathrm{old}}\Big)S_{\mu\nu}\Big]C_{\nu j}^{\mathrm{new}} \tag{2.8}$$

In this way, the full set of p_j values can be found by three matrix-vector multiplications, at $O(N^2)$ cost, and this adds negligibly to the cost of each SCF cycle. One then occupies the n orbitals with the largest projections p_j.

To use the MOM, the SCF calculation must begin with orbitals that lie within the basin of attraction of the target excited solution. Often, it is sufficient to perform a ground-state calculation and then simply promote an electron from an occupied to a virtual orbital. If this guess is sufficiently close to the target solution, the MOM will retain the excited configuration as the orbitals relax during the SCF. If, on the other hand, the guess lies outside of the basin of attraction, the SCF will converge to another solution of the same symmetry. In difficult cases, the quality of the guess may be improved by using orbitals that are optimal for the $(n - 1)$-electron system, or by using orbitals from another excited-state calculation.

An advantage of the MOM over other excited-state methods is that it is possible to single out a particular state without having to compute all lower energy states of the same symmetry. This could be useful, for example, when targeting excited states of a molecule in the presence of explicit solvent or when adsorbed onto a surface.[33] However, if several excitations are required, then we adopt a systematic approach to obtaining the states. Initial guesses are obtained by converging the ground state of the system and considering all single excitations of active electrons into low-lying virtual orbitals. Additional SCF calculations using each of these initial guesses are carried out using the MOM to converge the calculation to the solution closest to each guess. In this way, it is possible to obtain many excited states without requiring detailed knowledge of their electronic structure. This "black box" approach allows the MOM to be used in a similar way as CIS or TD-DFT.

Our approach is applicable to both HF and DFT calculations, the only difference being whether the one-electron operator $\hat{f}(\mathbf{r})$ in eq 1.2 includes the functional derivative of an exchange-

TABLE 1: Overlaps of the Seven Lowest Singlet HF/6-311+G(d) Solutions for the Alanine Molecule

ΔE (eV)	state	1 ^{1}A	2 ^{1}A	3 ^{1}A	4 ^{1}A	5 ^{1}A	6 ^{1}A	7 ^{1}A
4.60	2 ^{1}A	0.003	1					
5.51	3 ^{1}A	0.021	0.053	1				
6.81	4 ^{1}A	0.094	0.006	0.016	1			
6.83	5 ^{1}A	0.002	0.011	0.044	0.011	1		
7.01	6 ^{1}A	0.021	0.010	0.050	0.031	0.051	1	
7.28	7 ^{1}A	0.068	0.006	0.082	0.014	0.125	0.081	1

correlation density functional.[34] As a result, the MOM allows direct DFT calculations of excited states and thus offers a facile alternative to TD-DFT. The MOs obtained using the MOM can also be used in post-SCF methods, such as MP2, to model the correlation energy of the excited states. The computational cost of using the MOM is the same as that of the corresponding ground-state method (i.e., HF, DFT, or MP2) per excited state. This is the same as the conventional analogues CIS, TD-DFT, and CIS(D), however, an advantage of our approach is that the memory requirements remain constant and do not scale with the number of states.

3. Applications

The MOM has been implemented within the Q-Chem 3.0 package[35] and was used to generate the results in this section. Because excited-state electron densities can be much more diffuse than their ground-state analogues, it is important to use basis sets with added diffuse functions. In the case of DFT calculations (using either TD-DFT or MOM) it is also essential to use a quadrature grid that is large enough to integrate these diffuse densities.[36] All the DFT results in the following sections have employed the large EML-(100,194) grid for calculating exchange-correlation component of the energy.

3.1. Quasi-Orthogonality of SCF Solutions. As we noted above, the SCF solutions for a system are eigenfunctions of different operators and therefore cannot be expected to be strictly orthogonal. Nonetheless, it is interesting to examine empirically the extent to which such solutions are nearly orthogonal. The overlap between two HF wave functions represented in the same basis is

$$\langle \Psi_i^{\mathrm{HF}} | \Psi_j^{\mathrm{HF}} \rangle = \det(\mathbf{C}_i^{\dagger} \mathbf{S} \mathbf{C}_j) \tag{3.9}$$

where $\mathbf{C}_i$ and $\mathbf{C}_j$ are the corresponding occupied MO coefficient matrices. We have used this expression to calculate the overlaps between the first five singlet solutions for the alanine molecule at the HF/6-311+G(d)//MP2/cc-pVTZ level of theory, and these results are shown in Table 1. Alanine has C_1 symmetry, so all of the overlaps are nonzero, yet none exceeds 0.13. Although we do not artificially impose orthogonality on the states, we find that the solutions to the SCF equations are close to being orthogonal.

The nonzero overlap between the MOM states could lead to spurious enhancement of transition properties such as transition dipole moments (TDMs). To test whether or not this is the case, we have computed the TDMs and associated oscillator strengths for a selection of singlet transitions of the formamide molecule and show these in Table 2. The oscillator strengths show the transitions range from very weak to strong and show qualitative agreement between the MOM transitions and those predicted by CIS and TD-DFT. The A″ states are, of course, orthogonal to the ground state by symmetry; however, the HF 3 ^{1}A′ state shows significant overlap with the ground state (0.107). Despite this, the predicted transition moment is very similar to that predicted by B3LYP (which has a much lower overlap of 0.021) and both of these numbers lie within the range predicted by CIS and TD-DFT.

3.2. Atomic Excitation Energies. To begin our exploration of the MOM, we have used it to find ground- and excited-state HF solutions for a few small atoms, using the 6-311(3+,3+)G basis set.[37] (For helium, we used the same diffuse function exponents as for hydrogen.) The computed atomic excitation energies are compared with accurate experimental data[38] in Table 3.

We first used the MOM to find HF solutions for the 2s, 3s, and 4s configurations of the H atom. Because all of these share the spherical symmetry of the 1s ground-state configuration, they are almost impossible to find using the conventional aufbau protocol. The MOM, in contrast, locates them easily. HF theory is exact for one-electron systems, but only in the limit of a complete basis set, and our excitation energy errors (+0.00, +0.03, and +0.24 eV, respectively) therefore measure the quality of the basis set. We conclude from these errors that 6-311(3+,3+)G is satisfactory for the 2s and 3s configurations but inadequate for an accurate description of the 4s (and higher) configurations, which evidently require even more diffuse basis functions.

The ground-state configuration of the He atom is $1s^2$ and Table 3 shows results for all excitations in which one of the electrons is promoted to the 2s, 3s, or 4s orbital, to yield either a singlet (^{1}S) or triplet (^{3}S) state, and we see that all six of the HF excitation energies are too low by roughly 1.1 eV. How can this systematic underestimation be understood? Given a complete basis set, the only error in HF theory is its neglect of the correlation energy E_c and this will give rise to errors in excitation energies whenever the magnitude of E_c changes significantly between the initial and final states. In the ground state of helium, the two electrons are strongly correlated and $E_c = 1.14$ eV;[39] in any excited state where one of the electrons is promoted to another orbital, $E_c \approx 0$. Thus, whereas HF theory describes the excited states quite accurately, it gives an energy that is 1.14 eV too high for the ground state and thus underestimates the excitation energies by roughly the same amount.

The ground-state configuration of the Li atom is $1s^22s$, and Table 3 shows results for excitations in which the 2s electron is promoted to a 2p, 3s, or 3p orbital. On the basis of the results for the H and He atoms, and noting that the basis set quality is high and correlation effects should be small, we expect that the HF predictions for Li should be accurate. The results support this expectation.

The ground-state configuration of the Be atom is $1s^22s^2$, and Table 3 shows results for the single excitations in which one of the 2s electrons is promoted to a 2p or 3s orbital, and for the double excitations in which both 2s electrons are promoted into the 2p shell. In the case of the single excitations, the results are comparable to those for the He atom, correlation errors leading to systematic underestimation by more than 1 eV. The double excitation to the ^{3}P state gives a similar error (−0.96 eV) because, as in the single excitations, the strongly correlated $2s^2$ pair is broken by the excitation. However, in the doubly excited ^{1}D state, the two excited electrons remain strongly correlated and, as a result, the HF excitation energy (error = −0.15 eV) is much more accurate.

In the light of these prototypical atomic studies, we make two general observations:

1. Basis set errors, which are usually more pronounced for excited states than the ground state, tend to lead to overestimation of excitation energies (i.e., to positive errors);

TABLE 2: Transition Dipole Moments (a.u.), Oscillator Strengths, and Values of the Overlap with the Ground State for Selected Singlet Excited States of Formamide Using the 6-311(2+,2+)G(d,p) Basis[a]

state	excitation	theory	ΔE (eV)	overlap	μ_x	μ_y	μ_z	f
1 ^{1}A″	n → π^*	HF	4.25	0	0.000	0.000	−0.050	0.0003
		B3LYP	5.22	0	0.000	0.000	0.081	0.0008
		CIS	6.49	0	0.000	0.000	0.091	0.0013
		TD-DFT	5.57	0	0.000	0.000	0.080	0.0009
2 ^{1}A′[b]	$\pi \rightarrow \pi^*$	B3LYP	6.29	0.024	−1.323	−0.128	0.000	0.2723
		CIS	6.49	0	−0.916	−0.147	0.000	0.1879
		TD-DFT	7.99	0	0.791	0.048	0.000	0.1227
3 ^{1}A′	n → 3s	HF	5.78	0.107	−0.535	−0.170	0.000	0.0446
		B3LYP	6.62	0.021	−0.484	−0.077	0.000	0.0390
		CIS	9.65	0	0.561	0.092	0.000	0.0764
		TD-DFT	6.11	0	−0.319	−0.068	0.000	0.0159
2 ^{1}A″	$\pi \rightarrow$ 3s	HF	5.58	0	0.000	0.000	0.219	0.0066
		B3LYP	6.63	0	0.000	0.000	−0.228	0.0084
		CIS	7.69	0	0.000	0.000	0.325	0.0199
		TD-DFT	6.39	0	0.000	0.000	0.305	0.0145

[a] The TD-DFT results were computed using the B3LYP functional. [b] The HF $\pi \rightarrow \pi^*$ transition mixes significantly with the $\pi \rightarrow 3p_\pi$ transition and is not shown. Two states were obtained with ground-state overlaps of 0.069 and 0.005 and a combined oscillator strength of 0.1537; however, both showed considerable Rydberg character.

TABLE 3: Experimental and HF/6-311(3+,3+)G Excitation Energies (eV) of Atoms in Various Electron Configurations

atom	configuration[a]	term	expt[b]	HF	deviation	term	expt[b]	HF	deviation
H	2s	^{2}S	10.20	10.20	+0.00				
	3s	^{2}S	12.09	12.12	+0.03				
	4s	^{2}S	12.75	12.99	+0.24				
He	1s2s	^{3}S	19.82	18.74	−1.08	^{1}S	20.61	19.29	−1.32
	1s3s	^{3}S	22.72	21.60	−1.12	^{1}S	22.92	21.74	−1.18
	1s4s	^{3}S	23.59	22.49	−1.10	^{1}S	23.67	22.58	−1.09
Li	2p	^{2}P	1.85	1.84	−0.01				
	3s	^{2}S	3.37	3.34	−0.03				
	3p	^{2}P	3.83	3.80	−0.03				
Be	2s2p	^{3}P	2.73	1.67	−1.06	^{1}P	5.28	3.51	−1.77
	2s3s	^{3}S	6.46	5.33	−1.13	^{1}S	6.78	5.60	−1.18
	$2p^2$	^{3}P	7.40	6.44	−0.96	^{1}D	7.05	6.90	−0.15

[a] Valence electrons only. [b] Taken from the NIST webpage.[38]

TABLE 4: Deviations (eV) of Vertical Excitation Energies of Formaldehyde from Experimental Values

			conventional			MOM-based		
state	excitation	expt[a]	CIS	CIS(D)	TD-B3LYP	HF	MP2	B3LYP
$^3A_2$	n → π^*	3.50	+0.21	+0.04	−0.26	−1.05	+0.37	−0.16
$^3A_1$	$\pi \rightarrow \pi^*$	5.86	−1.07	+0.31	−0.09	−1.64	+0.35	+0.05
$^3B_2$	n → $3sa_1$	6.83	+1.47	−0.37	−0.46	−0.81	+0.60	+0.33
$^3B_2$	n → $3pa_1$	7.79	+1.28	−0.52	−0.62	−0.95	+0.46	+0.02
$^3A_1$	n → $3pb_2$	7.96	+1.76	−0.31	−0.50	−1.06	+0.45	+0.08
$^3A_2$	n → $3pb_1$	8.16	+1.15	−0.83	−1.01	−0.92	+0.52	+0.44
mean absolute deviation			1.16	0.40	0.49	1.07	0.46	0.18
$^1A_2$	n → π^*	4.07	+0.46	−0.04	−0.15	−1.51	+0.03	−0.58
$^1B_2$	n → $3sa_1$	7.11	+1.51	−0.67	−0.64	−1.08	+0.37	+0.10
$^1B_2$	n → $3pa_1$	7.97	+1.40	−0.71	−0.74	−1.08	+0.35	−0.10
$^1A_1$	n → $3pb_2$	8.14	+1.62	−0.66	−0.95	−1.24	+0.30	−0.06
$^1A_2$	n → $3pb_1$	8.37	+1.13	−0.38	−0.92	−1.19	+0.33	+0.20
mean absolute deviation			1.22	0.49	0.68	1.22	0.27	0.21

[a] Reference 40.

2. Correlation errors, for excitations in which an electron pair is broken, tend to lead to underestimation of excitation energies (i.e., to negative errors).

3.3. Molecular Excitation Energies. Tables 4−7 show errors in a variety of vertical excitation energies of formaldehyde, ethylene, acetaldehyde, and acetone at the HF, MP2, and B3LYP levels, using the MOM to obtain the single-determinant wave functions of the excited states. We also include excitation energies computed at the conventional CIS, CIS(D), and TD-B3LYP levels. All energies were computed using the 6-311(2+,2+)G(d,p) basis set at MP2/cc-pVTZ optimized geometries. The errors are computed with respect to the experimental values.[40−42] The overall mean absolute deviation (MAD) of each level is summarized in Table 8.

The large MADs of CIS and HF (1.01 and 1.14 eV, respectively) are unsurprising given that these methods ignore electron correlation. As noted above, for excitations that involve the breaking of an electron pair, HF systematically underestimates the excitation energy by approximately the pair correlation energy, and we observe that the HF errors are close to E_c for the helium atom. In contrast, CIS frequently overestimates

TABLE 5: Deviations (eV) of Vertical Excitation Energies of Ethylene from Experimental Values

			conventional			mom-based		
state	excitation	expt[a]	CIS	CIS(D)	TD-B3LYP	HF	MP2	B3LYP
$^3B_{1u}$	$\pi \rightarrow \pi^*$	4.30	−0.67	+0.31	+0.16	−0.92	+0.30	+0.16
$^3B_{3u}$	$\pi \rightarrow 3s$	6.98	−0.05	+0.15	−0.44	−1.10	+0.27	+0.01
^3A_g	$\pi \rightarrow 3p\pi$	8.15	−0.37	−0.05	−0.77	−1.44	+0.08	−0.18
mean absolute deviation			0.36	0.17	0.46	1.15	0.22	0.12
$^1B_{1u}$	$\pi \rightarrow \pi^*$	7.65	+0.13	+0.43	+0.02	−1.31	−1.41	−1.84
$^1B_{3u}$	$\pi \rightarrow 3s$	7.11	+0.03	+0.12	−0.50	−1.17	+0.21	−0.08
$^1B_{1g}$	$\pi \rightarrow 3p\sigma$	7.80	−0.07	+0.07	−0.68	−1.23	+0.21	−0.21
^1A_g	$\pi \rightarrow 3p\pi$	8.26	−0.15	−0.07	−0.80	−1.38	+0.03	−0.23
mean absolute deviation			0.09	0.17	0.50	1.27	0.46	0.59

[a] Taken from ref 41.

TABLE 6: Deviations (eV) of Vertical Excitation Energies of Acetaldehyde from Experimental Values

			conventional			MOM-based		
state	excitation	expt[a]	CIS	CIS(D)	TD-B3LYP	HF	MP2	B3LYP
$^3A''$	$n \rightarrow \pi^*$	3.97	+0.20	−0.07	−0.33	−1.13	+0.31	−0.32
$^3A'$	$\pi \rightarrow \pi^*$	5.99	−0.86	+0.34	−0.13	−1.52	+0.43	+0.62
$^3A'$	$n \rightarrow 3s$	6.81	+1.40	−0.63	−0.72	−1.03	+0.38	+0.35
$^3A'$	$n \rightarrow 3p_x$	7.44	+1.45	−0.57	−0.81	−0.80	+0.67	+0.05
$^3A'$	$n \rightarrow 3p_y$	7.80	+1.46	−0.78	−0.47	−1.33	+0.09	+0.28
mean absolute deviation			1.07	0.48	0.49	1.16	0.38	0.32
$^1A''$	$n \rightarrow \pi^*$	4.28	+0.65	+0.06	−0.02	−1.34	+0.22	−0.49
$^1A'$	$n \rightarrow 3s$	6.82	+1.65	−0.68	−0.61	−0.99	+0.42	−0.17
$^1A'$	$n \rightarrow 3p_y$	7.46	+1.73	−0.62	−0.76	−0.96	+0.47	−0.25
$^1A'$	$n \rightarrow 3p_x$	7.75	+1.53	−0.41	−0.77	−1.05	+0.39	−0.23
mean absolute deviation			1.39	0.44	0.54	1.09	0.37	0.28

[a] Taken from ref 40.

TABLE 7: Deviations (eV) of Vertical Excitation Energies of Acetone from Experimental Values

			conventional			MOM-based		
state	excitation	expt[a]	CIS	CIS(D)	TD-B3LYP	HF	MP2	B3LYP
$^3A_2$	$n \rightarrow \pi^*$	4.16	+0.30	−0.07	−0.34	−1.10	+0.34	−0.32
$^3A_1$	$\pi \rightarrow \pi^*$	5.88	−0.53	+0.52	+0.03	−1.26	+0.65	+0.13
mean absolute deviation			0.42	0.30	0.19	1.18	0.49	0.23
$^1A_2$	$n \rightarrow \pi^*$	4.38	+0.81	+0.10	+0.03	−1.24	+0.32	−0.41
$^1B_2$	$n \rightarrow 3s$	6.35	+1.90	−0.64	−0.59	−0.81	+0.51	−0.14
$^1A_1$	$n \rightarrow 3p_y$	7.41	+1.64	−0.92	−0.88	−1.01	+0.41	−0.29
$^1A_2$	$n \rightarrow 3p_x$	7.36	+1.82	−0.62	−0.75	−1.11	+0.41	—[b]
$^1B_2$	$n \rightarrow 3p_z$	7.45	+1.71	−0.93	−0.76	−1.11	+0.39	−0.23
mean absolute deviation			1.58	0.64	0.60	1.06	0.41	0.27

[a] Taken from ref 42. [b] State could not be obtained using the 6-311(2+,2+)G(d,p) basis set.

TABLE 8: Mean Absolute Deviations of the Excitation Energies for Formaldehyde, Ethylene, Acetaldehyde, and Acetone

	conventional			MOM-based		
MAD	CIS	CIS(D)	TD-B3LYP	HF	MP2	B3LYP
singlets	1.11	0.45	0.59	1.15	0.38	0.33
triplets	0.89	0.37	0.45	1.13	0.39	0.22
all	1.01	0.41	0.52	1.14	0.38	0.28

excitation energies because it does not allow the excited-state orbitals to relax and is consequently unbalanced.

The excitation energies from TD-B3LYP are significantly closer to experiment, and their average deviation (0.52 eV) is similar to that reported by Hirao et al.[43] TD-DFT usually underestimates the excitation energies of diffuse or Rydberg states because the asymptotic behavior of the exchange-correlation potential is incorrect. On average, the MOM-based B3LYP excitation energies (MAD = 0.28 eV) are significantly more accurate than the TD-B3LYP values (MAD = 0.52 eV) and this is a consequence of the much improved modeling of the Rydberg states. The TD-DFT description of Rydberg states can be improved through asymptotically corrected functionals, and various schemes have been proposed for this,[16,43−45] but our B3LYP results are in closer agreement with experiment than even the long-range-corrected BLYP functional.[43]

Overall, the MOM-based approaches provide comparable accuracy to the corresponding response-based methods, CIS, CIS(D) and TD-B3LYP. The largest MOM errors arise for the $^1B_{1u}$ ($\pi \rightarrow \pi^*$) state of ethylene, where the MP2 and B3LYP excitation energies are too low by 1.41 and 1.84 eV, respectively. The errors for the corresponding triplet excitation are only 0.30 and 0.16 eV and the source of the error for the singlet can be understood as follows. A single-determinant wave function for an open-shell singlet is a mixture of the triplet state and the true singlet state, and the associated excitation energy lies between the excitation energy of the triplet state and the true singlet state. Consequently, excitation energies for singlet states will be underestimated by approximately half of the energy difference between the respective singlet and triplet states. For

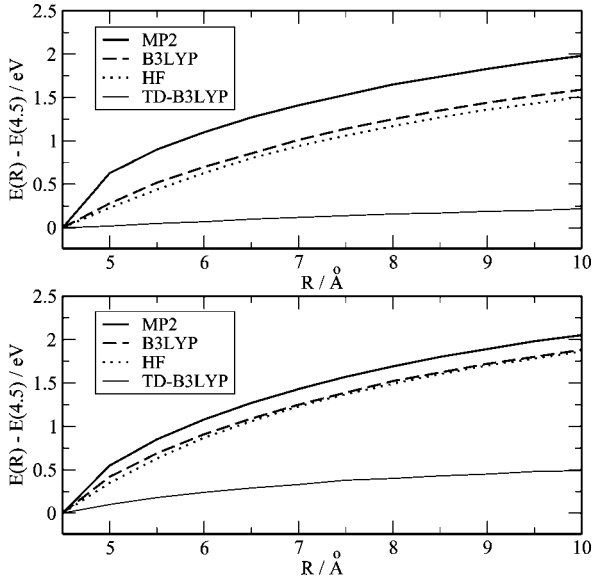

Figure 1. Variation of the $\pi C_2F_4 \rightarrow \pi C_2{}^*H_4$ (lower panel) and $\pi C_2H_4 \rightarrow \pi C_2F_4{}^*$ (top panel) excitation energies of the $C_2H_4 \cdots C_2F_4$ complex with intermolecular separation R. The following shifts (in eV) were applied so that the curves intersect at $R = 4.5$ Å. Upper panel: HF, −10.02; B3LYP, −11.19; MP2, −11.34; TD-B3LYP, −7.58. Lower panel: HF, −10.35; B3LYP, −10.01; MP2, −10.53; TD-B3LYP, −6.63.

the $^1B_{1u}$ of ethylene, the triplet state lies 3.35 eV below the singlet state, consistent with the 1.41 eV error by MP2.

The B3LYP energy for the second $^1A_2$ state of acetone (Table 7) could not be obtained, and this illustrates the key difficulty that one faces when using the MOM protocol. Several different sets of initial guess orbitals were used to try to capture this state but, in each case, the SCF converged to the lower-energy $^1A_2$ ($n \rightarrow \pi^*$) state, indicating that the basin of attraction for the higher state is very small for the 6-311(2+,2+)G(d,p) basis set. Curiously, however, the higher state can easily be obtained with the smaller 6-311(2+)G(d) basis, and was found to lie 7.56 eV above the ground state.

3.4. Charge Transfer Excitations. The failure of TD-DFT with standard functionals to provide a satisfactory treatment of charge-transfer states is a well-known problem.[46−48] For such states, TD-DFT underestimates the excitation energy substantially and fails to yield the correct $1/R$ dependence of the charge-transfer states, where R denotes the separation between the charges. Recent work has traced this deficiency to the absence of exact nonlocal exchange.[19,20] In a charge-transfer excitation, the electron-donating orbital ψ_i and electron-accepting orbital ψ_a have very little overlap and, because of the self-interaction error present in approximate exchange-correlation potentials, the electron in ψ_a interacts spuriously with itself in ψ_i. Several groups have proposed schemes to address this problem; Dreuw and Head-Gordon used a hybrid approach that combines TD-DFT and CIS,[20] Tawanda et al. obtained the correct $1/R$ dependence by using a long-range corrected functional[43] and, recently, Zhao and Truhlar introduced an exchange-correlation functional that contains full HF exchange.[49]

MOM-based calculations of excited charge-transfer states do not suffer from the electron-transfer self-interaction problem, and thus offer a promising route to the study of charge-transfer states within DFT. Furthermore, such states can also be studied using MOM-based HF and MP2 theory. Figure 1 shows the variation of the $\pi C_2H_4 \rightarrow \pi C_2F_4{}^*$ and $\pi C_2F_4 \rightarrow \pi C_2H_4{}^*$ charge-transfer excitations in an ethylene/tetrafluoroethylene complex as a function of the intermolecular separation R, computed using HF, MP2, B3LYP, and TD-B3LYP with the 6-31G(d) basis set. As found elsewhere,[19] TD-DFT predicts that the excitation energy is simply the energy difference between the electron-donating and electron-accepting orbitals and is therefore almost independent of R. In contrast, HF, MP2, and B3LYP all show the correct $1/R$ dependence for both excitations.

TABLE 9: Optimized Structural Parameters for the Given States of Formaldehyde

state	parameter	acc[a]	HF	MP2	B3LYP
(G.S.)[b]	r(C−O) (Å)	1.203	1.180	1.212	1.202
	r(C−H) (Å)	1.101	1.094	1.104	1.108
	∠HCH (deg)	116.3	116.1	116.0	116.0
	∠OOP[c] (deg)	0.0	0.0	0.0	0.0
$^1A''$ ($n \rightarrow \pi^*$)[b]	r(C−O) (Å)	1.323	1.340	1.328	1.310
	r(C−H) (Å)	1.098	1.079	1.090	1.099
	∠HCH (deg)	118.8	119.6	118.4	115.7
	∠OOP (deg)	34.0	35.4	37.3	37.9
$^1A_1$ ($\pi \rightarrow \pi^*$)[d]	r(C−O) (Å)	1.583	1.393	1.459	1.453
	r(C−H) (Å)	1.095	1.075	1.082	1.084
	∠HCH (deg)	119.6	121.3	125.8	123.1
	∠OOP (deg)	0.0	0.0	0.0	0.0
$^1B_2$ ($n \rightarrow 3sa_1$)[d]	r(C−O) (Å)	1.198	1.206	1.194	1.206
	r(C−H) (Å)	1.131	1.102	1.141	1.378
	∠HCH (deg)	120.7	123.9	124.9	167.2
	∠OOP (deg)	0.0	0.0	0.0	0.0

[a] Accurate values taken from ref 53. [b] Experimental values. [c] Out-of-plane angle. [d] EOM-CCSD values.

3.5. Structure and Spectroscopy of Excited States. Theoretical methods for determining the equilibrium structures and vibrational frequencies of molecular ground states are well developed. Efficient optimization of molecular structures requires analytical first derivatives of the energy and, through additional programming effort, these derivatives have become available for excited-state methods such as CIS,[13] TD-DFT,[50] CASPT2,[51] and EOM-CCSD.[52] An advantage of computing excited states within the MOM framework is that ground-state code can be applied directly to excited states. This provides a computationally inexpensive approach for determining excited-state structures without the need for additional programming effort. Likewise, ground-state methods whose analytical second derivatives are available can be applied to compute vibrational frequencies for excited states.

Table 9 shows the optimized geometric parameters for the ground and three low-lying excited states of formaldehyde obtained using the MOM approach with HF, MP2, and B3LYP. Experimental values (where available) or accurate EOM-CCSD values are also shown for comparison. All three approaches give very accurate predictions of the ground-state structure and there is only a slight degradation in performance of HF and MP2 for the $^1A''$ ($n \rightarrow \pi^*$) and $^1B_2$ ($n \rightarrow 3sa_1$) excited states. B3LYP completely fails to capture the $^1B_2$ state, predicting an almost linear H−C−H angle, and it also has the worst predictions for the $^1A''$ state. All three theories give good values for the C−O bond lengths in these two states, and predict the correct nonplanar structure for the $^1A''$ state, although the out-of-plane angle is slightly overestimated in each case.

The computed geometries are poorest for the $^1A_1$ ($\pi \rightarrow \pi^*$) state with all three methods significantly underestimating the C−O bond length. It was noted in Section 3.3 that single-determinant methods perform poorly for open-shell singlets where the singlet−triplet gap is large. This is the case for the $\pi \rightarrow \pi^*$ transition in formaldehyde where the gap is approximately 4 eV. The C−O bond length in the singlet (1.583

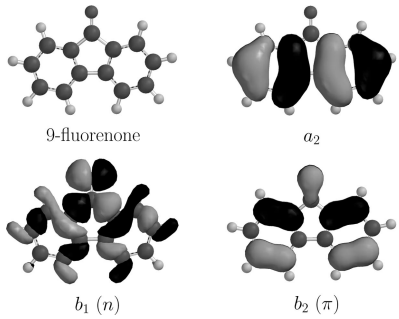

Figure 2. Molecular orbitals and nuclear framework of 9-fluorenone.

Å[53]) is very different from that in the triplet (1.423 Å[54]) and we see that the MP2 and B3LYP bond lengths fall between these two values, reflecting the mixing of the two spin states that occurs in the single-determinant treatment of an open-shell singlet.

The availability of analytic second derivatives for HF and DFT methods allows harmonic vibrational frequencies to be computed for the MOM-based excited states of large systems. Time-resolved infrared spectroscopy is used to measure the infrared spectroscopy of excited states and calculations can often assist in the interpretation of the spectra obtained. Aromatic carbonyl compounds have diverse photophysical and photochemical properties arising from the close proximity of the singlet and triplet n $\rightarrow \pi^*$ and $\pi \rightarrow \pi^*$ transitions.[55] IR spectra have been measured for the S_1 and T_1 states of fluorenone,[56] and these show the CO stretch frequency to be 1600 cm^{-1} in the T_1 state, with weaker bands at 1516 and 1476 cm^{-1}, while in the S_1 state the CO stretch frequency is at 1544 cm^{-1}, with weaker bands at 1496 and 1400 cm^{-1}. These results indicate that both the S_1 and T_1 states are of $\pi \rightarrow \pi^*$ character. Figure 2 shows the structure and relevant molecular orbitals of fluorenone with symmetry classifications within the C_{2v} point group. A number of low-lying excited states can be generated by the excitations $18b_1 \rightarrow 5b_2$, $3a_2 \rightarrow 5b_2$, and $4b_2 \rightarrow 5b_2$. In more familiar notation, the $5b_2$ orbital can be regarded as the π^* orbital, and the $18b_1$ and $4b_2$ are n and π in character. The $3a_2$ orbital also has π character and is located on the rings. The three excited states can be denoted nπ^*, $a_2\pi^*$, and $\pi\pi^*$, respectively.

The MOM allows the IR spectrum for arbitrary excited states to be evaluated and, through comparison of the computed spectra with experiment, the nature of the excited-state determined. We have computed the IR spectra for the triplet and singlet $a_2\pi^*$, nπ^*, and $\pi\pi^*$ excited states of fluorenone. The frequencies were computed using B3LYP/6-31G(d) and were scaled by 0.9614.[57] The spectra were generated by representing each vibrational frequency by a Gaussian function, with the bandwidth determined by the computed intensity. Bandwidths of 2, 3, 4, 5, and 6 cm^{-1} were used for intensities in the ranges <10, $10-20$, $20-30$, $30-150$, and >150 km mol^{-1}, respectively, since these were found to give the best graphical agreement with the experimental results. The resulting spectra are shown in Figure 3.

The computed spectra for the three triplet states are all significantly different. The experimental spectrum agrees well with the computed spectrum for the $^3a_2\pi^*$ state but not those for the ^{3}nπ^* or $^3\pi\pi^*$ states. In particular, the computed CO stretching frequency (1598 cm^{-1}) in the $^3a_2\pi^*$ state almost exactly matches the experimental value (1600 cm^{-1}), indicating that the lowest triplet state involves an $a_2 \rightarrow \pi^*$ excitation. A similar analysis for the excited singlet states shows that the lowest singlet is also an $a_2 \rightarrow \pi^*$ state and the computed CO stretch (1552 cm^{-1}) compares well with the experimental value (1544 cm^{-1}).

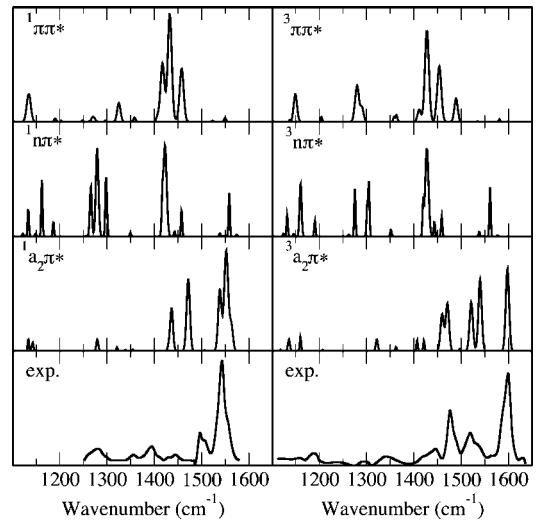

Figure 3. Computed IR spectra for the singlet and triplet excited states of 9-fluorenone.

4. Conclusions

We have introduced a simple strategy that yields excited-state solutions of SCF equations by using a novel method for determining which orbitals to occupy on each SCF cycle. The excitation energies computed using our method with the HF, MP2, and B3LYP levels of theory are competitive with their conventional analogues, CIS, CIS(D), and TD-DFT. Furthermore, our approach has several advantages over these conventional methods; it is easy to implement, it inherits the analytic energy derivatives from ground-state theory, and it yields a simple single-determinant wave function and density that are easy to interpret.

Acknowledgment. We thank the late Prof. John A. Pople for his insightful comments on the theory of the MOM in the early stages of this work. We also thank Prof. Michael W. George for useful discussions on the vibrational spectra of 9-fluorenone. N.A.B. is grateful to the ANU for a 2007 Visiting Fellowship and to the EPSRC for an Advanced Research Fellowship.

References and Notes

(1) Hartree, D. R. *Proc. Cambridge Philos. Soc.* **1928**, *24*, 89.
(2) Fock, V. *Z. Phys.* **1930**, *61*, 126.
(3) Hohenberg, P.; Kohn, W. *Phys. Rev.* **1964**, *136*, B864.
(4) Kohn, W.; Sham, L. J. *Phys. Rev.* **1965**, *140*, A1133.
(5) Szabo, A.; Ostlund, N. S. *Modern Quantum Chemistry*; McGraw-Hill: New York, 1989.
(6) Roothaan, C. C. J. *Rev. Mod. Phys.* **1951**, *23*, 69.
(7) Saunders, V. R.; Hillier, I. H. *Int. J. Quantum Chem.* **1973**, *7*, 699.
(8) Seeger, R.; Pople, J. A. *J. Chem. Phys.* **1976**, *65*, 265.
(9) Bacskay, G. B. *Chem. Phys.* **1981**, *61*, 385.
(10) Pulay, P. *J. Comput. Chem.* **1982**, *3*, 556.
(11) van Voorhis, T.; Head-Gordon, M. *Mol. Phys.* **2002**, *100*, 1713.
(12) Del Bene, J. E.; Ditchfield, R.; Pople, J. A. *J. Chem. Phys.* **1971**, *55*, 2236.
(13) Foresman, J. B.; Head-Gordon, M.; Pople, J. A.; Frisch, M. J. *J. Chem. Phys.* **1992**, *96*, 135.
(14) Runge, E.; Gross, E. K. U. *Phys. Rev. Lett.* **1984**, *52*, 997.
(15) Casida, M. E. *Recent Advances in Density Functional Methods, Part I*; World Scientific: Singapore, 1995.
(16) Tozer, D. J.; Handy, N. C. *J. Chem. Phys.* **1998**, *109*, 10180.

(17) Casida, M. E.; Salahub, D. R. *J. Chem. Phys.* **2000**, *113*, 8918.
(18) Tozer, D. J.; Handy, N. C. *Mol. Phys.* **2003**, *101*, 2669.
(19) Dreuw, A.; Weisman, J.; Head-Gordon, M. *J. Chem. Phys.* **2003**, *119*, 2943.
(20) Dreuw, A.; Head-Gordon, M. *J. Am. Chem. Soc.* **2004**, *126*, 4007.
(21) Andersson, K.; Malmqvist, P.-Å.; Roos, B. O.; Sadlej, A. J.; Wolinski, K. *J. Phys. Chem.* **1990**, *94*, 5483.
(22) Andersson, K.; Malmqvist, P.-Å.; Roos, B. O. *J. Chem. Phys.* **1990**, *96*, 1218.
(23) Stanton, J. F.; Bartlett, R. J. *J. Chem. Phys.* **1993**, *98*, 7029.
(24) Krylov, A. I. *Chem. Phys. Lett.* **2001**, *338*, 375.
(25) Hunt, W. J.; Goddard, W. A., III *Chem. Phys. Lett.* **1969**, *3*, 414.
(26) Huzinaga, S.; Arnau, C. *J. Chem. Phys.* **1971**, *54*, 1948.
(27) Huzinaga, S.; Arnau, C. *Phys. Rev. A* **1970**, *1*, 1285.
(28) Morokuma, K.; Iwata, S. *Chem. Phys. Lett.* **1972**, *16*, 192.
(29) Gidopoulos, N. I.; Papaconstantinou, P. G.; Gross, E. K. U. *Physica B* **2002**, *318*, 328.
(30) Lions, P. *Commun. Math. Phys.* **1987**, *109*, 33.
(31) Stanton, R. E. *J. Chem. Phys.* **1968**, *48*, 257.
(32) Sears, J. S.; Sherrill, C. D. *J. Chem. Phys.* **2006**, *124*, 144314.
(33) Besley, N. A. *Chem. Phys. Lett.* **2004**, *390*, 124.
(34) Pople, J. A.; Gill, P. M. W.; Johnson, B. G. *Chem. Phys. Lett.* **1992**, *199*, 557.
(35) Shao, Y.; Molnar, L. F.; Jung, Y.; Kussmann, J.; Ochsenfeld, C.; Brown, S. T.; Gilbert, A. T. B.; Slipchenko, L. V.; Levchenko, S. V.; O'Neill, D. P.; DiStasio Jr, R. A.; Lochan, R. C.; Wang, T.; Beran, G. J. O.; Besley, N. A.; Herbert, J. M.; Lin, C. Y.; Voorhis, T. V.; Chien, S.-H.; Sodt, A.; Steele, R. P.; Rassolov, V. A.; Maslen, P. E.; Korambath, P. P.; Adamson, R. D.; Austin, B.; Baker, J.; Byrd, E. F. C.; Dachsel, H.; Doerksen, R. J.; Dreuw, A.; Dunietz, B. D.; Dutoi, A. D.; Furlani, T. R.; Gwaltney, S. R.; Heyden, A.; Hirata, S.; Hsu, C.-P.; Kedziora, G.; Khalliulin, R. Z.; Klunzinger, P.; Lee, A. M.; Lee, M. S.; Liang, W.; Lotan, I.; Nair, N.; Peters, B.; Proynov, E. I.; Pieniazek, P. A.; Rhee, Y. M.; Ritchie, J.; Rosta, E.; Sherrill, C. D.; Simmonett, A. C.; Subotnik, J. E.; Woodcock III, H. L.; Zhang, W.; Bell, A. T.; Chakraborty, A. K.; Chipman, D. M.; Keil, F. J.; Warshel, A.; Hehre, W. J.; Schaefer III, H. F.; Kong, J.; Krylov, A. I.; Gill, P. M. W.; Head-Gordon, M. *Phys. Chem. Chem. Phys.* **2006**, *8*, 3172.
(36) Gräfenstein, J.; Cremer, D. *J. Chem. Phys.* **2007**, *127*, 164113.
(37) Wong, M. W.; Gill, P. M. W.; Nobes, R. H.; Radom, L. *J. Phys. Chem.* **1988**, *92*, 4875.
(38) http://physics.nist.gov/PhysRefData/ASD.
(39) Davidson, E.; Hagstrom, S.; Chakravorty, S.; Umar, V.; Fischer, C. F. *Phys. Rev. A* **1991**, *44*, 7071.
(40) Robin, M. B. *Higher Excited States of Polyatomic Molecules*; Academic Press: New York, 1985.
(41) Palmer, M. H.; Beveridge, A. J.; Walker, I. C.; Abuain, T. *Chem. Phys.* **1986**, *102*, 63.
(42) Merchán, M.; Roos, B. O.; McDiarmid, R.; Xing, X. *J. Chem. Phys.* **1996**, *104*, 1791.
(43) Tawanda, Y.; Tsuneda, T.; Yanagisawa, S.; Yanai, T.; Hirao, K. *J. Chem. Phys.* **2004**, *120*, 8425.
(44) van Leeuwen, R.; Baerends, E. *J. Phys. Rev. A* **1994**, *49*, 2421.
(45) Tozer, D. J. *J. Chem. Phys.* **1999**, *112*, 3507.
(46) Tozer, D. J.; Amos, R. D.; Handy, N. C.; Roos, B. J.; Serrano-Andres, L. *Mol. Phys.* **1999**, *97*, 859.
(47) Sobolewski, A. L.; Domcke, W. *Chem. Phys.* **2003**, *294*, 73.
(48) Dreuw, A.; Fleming, G. R.; Head-Gordon, M. *J. Phys. Chem. B* **2003**, *107*, 6500.
(49) Zhao, Y.; Truhlar, D. G. *J. Phys. Chem. A* **2006**, *110*, 13126.
(50) Furche, F.; Ahlrichs, R. *J. Chem. Phys.* **2002**, *117*, 7433.
(51) Celani, P.; Werner, H.-J. *J. Chem. Phys.* **2003**, *119*, 5044.
(52) Stanton, J. F.; Gauss, J. *J. Chem. Phys.* **1994**, *100*, 4695.
(53) Wiberg, K. B.; de Oliveira, A. E.; Trucks, G. *J. Phys. Chem.* **2002**, *106*, 4192.
(54) Taylor, S.; Wilden, D. G.; Comer, J. *Chem. Phys.* **1982**, *70*, 291.
(55) Turro, N. J. *Modern Molecular Photochemistry*; Benjamin-Cummings: Menlo Park, CA, 1978.
(56) Tanaka, S.; Kato, C.; Horie, K.; Hamaguchi, H. *Chem. Phys. Lett.* **2003**, *381*, 385.
(57) Scott, A. P.; Radom, L. *J. Phys. Chem.* **1996**, *100*, 16502.

JP801738F